International Journal of High-Rise Buildings
September 2016, Vol 5, No 3, 155-165
http://dx.doi.org/10.21022/IJHRB.2016.5.3.155

International Journal of
High-Rise Buildings
www.ctbuh-korea.org/ijhrb/index.php

Performance of Seismic Protective Systems for Super-Tall Buildings and Their Contents

Kazuhiko Kasai†

Tokyo Institute of Technoogy, Nagatsuta, Yokohama 226-8503, Japan

Abstract

A much higher level of seismic performance is needed for supertall buildings due to increased demands for their functional continuities and the recognized needs for their continuing emergence in metropolitan areas. This paper analyzes, compares, and contrasts responses recorded during the 2011 Tohoku-oki Earthquake of different supertall buildings featuring conventional and vibration-controlled engineering systems. The superior performance and advantage of the latter are pointed out, and the typical dynamic properties, response characteristics, and effects on the secondary system are discussed. Ongoing efforts to enhance vibration control performance are described, covering the development of specifications, use of performance curves and targeted displacement design, and methods to find appropriate locations of damper installation resulting in a minimized amount of dampers.

Keywords: Super-Tall buildings, Protective systems, Vibtation control, Dampers, Monitoring, Displacement and Acceleration Response, Performance curve, Displacement-targeted design, Tohoku-Oki Earthquake

1. Introduction

1.1. Protective Systems

As the modern society has become more complex and hence vulnerable to seismic hazards, the risk of a major city in a seismically active area has increased drastically. In addition to the traditional code-based design approach aiming to protect human lives while accepting the building damage, design to assure enhanced performance of protecting socio-economic values of the building needs to be addressed.

This is especially true for the super-tall buildings, since the loss of their function can cause enormous impact to the area and society. The Japanese super-tall building constructed recently, therefore, employs the protective system, either vibration-controlled system or base-isolated system. Compared with the conventional structural system, they can control both displacements and accelerations of the buildings, thereby better protecting the structural/non-structural components as well as building contents.

1.2. Seismic Protection of Super-Tall Buildings

The 1995 Kobe earthquake indicated importance of keeping building damage small enough to allow post-quake use of the building, and promoted accelerated use of the protective systems (JSSI, 2003, 2005, 2007, 2013). However, its frequency contents were not very threatening to the super-tall buildings. The 2003 Tokachi-Oki earthquake, and the 2004 Chuetsu and 2007 Chuetsu-Oki earthquakes caused long period shaking in Tokyo. During the 2011 Tohoku-Oki earthquake that caused tremendous tsunami disaster, shaking was the strongest ever for the modern buildings in Tokyo located over 300 km away from the epicenter. It had wide range of frequency contents (Kasai et al., 2013), and excited low to higher modes of the super-tall buildings, containing the long period shaking stronger than the 2004 and 2007 events. The ground acceleration was 0.5 to 1.5 m/s^2, but 3 to 4 times stronger shaking is expected in the near future.

Since the public transportations were shut down for over 24 hours, most commuter workers could not return home (Fig. 1(a)), resulting in the recognized needs for super-tall buildings not to produce many evacuees but to become havens for the commuters (Fig. 1(b)).

1.3. Objectives and Scopes

The objectives of this paper, therefore, are to validate



(a) Shinjuku station entrance (b) Lobby of Kougakuin Univ. bldg.

Figure 1. Impact of Tohoku-oki earthquake in Tokyo (From Profs. Hisada & Yamashita, Kogakuin Univ.).

†Corresponding author: Kazuhiko Kasai
Tel: +81-45-924-5512; Fax: +81-45-924-5525
E-mail: kasai.k.ac@m.titech.ac.jp

effectiveness of protective systems for the super-tall buildings based on the records obtained during the 2011 quake, and to explain Japan's development of design and codifications for better performance of the systems, including cases for retrofit. The paper mainly refers to the vibration-controlled systems, since they are typical protective systems for super-tall buildings.

Sec. 2 discusses effectiveness of the vibration-controlled systems based on the responses recorded during the 2011 Tohoku-Oki earthquake. Dynamic properties such as damping ratios and time-history responses are contrasted with those of conventional structural systems. Sec. 3 explains Japan's progress in specifications and design methods for the protective systems, including those developed by the writer and his colleagues. A variety of methods for evaluating the dynamic characteristics and predicting the maximum responses are explained.

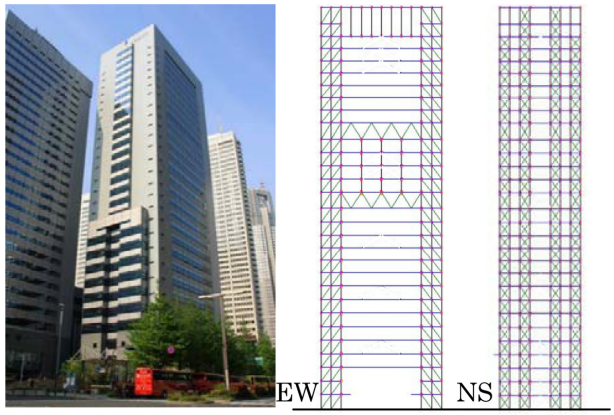
2. Super-Tall Buildings and Response Records

2.1. Building with Conventional Structure

The example is a seismically-resistant 29-story steel building (Fig. 2) constructed in 1989. It is a school building of Kogakuin University (Hisada et al., 2012; Kasai et al., 2012), located in central Tokyo. The building height is 143 m, floor plan dimension is 38.4 and 25.6 m in EW (x-) and NS (y-) directions, respectively, and steel moment resisting frame combined with many short braces provided seismic resistance (Fig. 2(b)). By promptly checking the response records, the Kogakuin professors considered the structure undamaged, and let about 700 non-university people stay in the first floor lobby of the building (Fig. 1(b)).

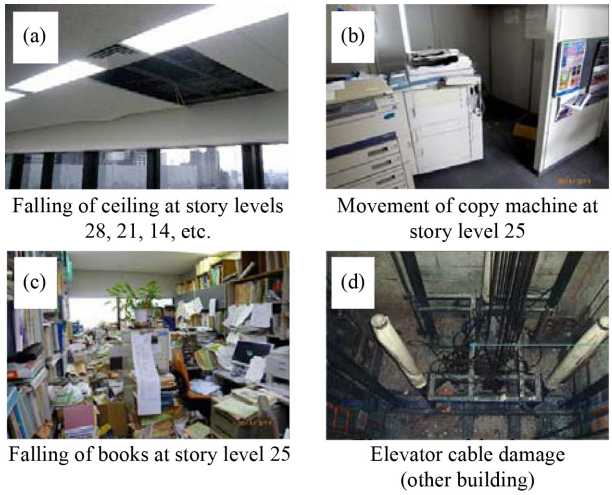
On the other hand, ceiling partially fell down (Fig. 3(a)) in the mid- and upper stories, implying short period acceleration input on those stories. In contrast, the copy machine with casters (Fig. 3(b)), presumably having a long vibration period, moved over and impacted other equipment, implying long period acceleration there. High accelerations also caused falling of books from shelves (Fig. 3(c)). In a nearby super-tall building, elevator cables were damaged (Fig. 3(d)), possibly resonating to the long period accelerations, and it took three weeks until the elevator was back to service. Similar failures occurred due to the long period shaking by the 2004 Chuetsu earthquake. Previously, little attention was paid to the acceleration-induced damage which, however, can become enormous for the future shaking 3 to 4 times stronger.

During the 2011 Tohoku-Oki earthquake, the peak accelerations in x- and y-directions were 0.91 and 0.89 m/s^2 at the base, and 2.35 and 3.16 m/s^2 at the top floor, respectively. The average drift angle, top floor displacement divided by the height, is 1/350 rad, and the structure remained elastic. Fig. 4(a) compares acceleration records at base and top floor in y-direction. The earthquake duration is long and about 200 seconds. For the first 90 seconds of



(a) 29-story building (b) EW (X) and NS (Y) frames

Figure 2. Super-tall building in central Tokyo.



Falling of ceiling at story levels 28, 21, 14, etc.

Movement of copy machine at story level 25

Falling of books at story level 25

Elevator cable damage (other building)

Figure 3. Acceleration-induced damage.

the figure, short period accelerations of the base and top floor are apparent. For the next 110 seconds, long period and very weak base accelerations as well as largely amplified top floor accelerations are seen (Fig. 4(b)).

By using the transfer function (Sec. 2.2), the vibration periods for the first three modes are 2.96 s, 1.00 s, and 0.52 s for x-direction, and 3.10 s, 0.94 s, and 0.47 s for y-direction, respectively. Likewise, damping ratios are 0.017, 0.018, and 0.034 for x-direction, and 0.021, 0.016, and 0.034 for y-direction, respectively. Damping ratio 0.01 was estimated from small amplitude vibration tests before 2011 (Hisada, 2011).

Using the above modal properties and participation vectors estimated, contribution of each vibration mode is obtained with excellent accuracy (Kasai et al., 2013; Kasai et al., 2012). Fig. 4(b) shows that the acceleration of each mode at the top floor is dominated by the 2nd mode for the first 90 seconds. For the later 110 seconds, the 1st

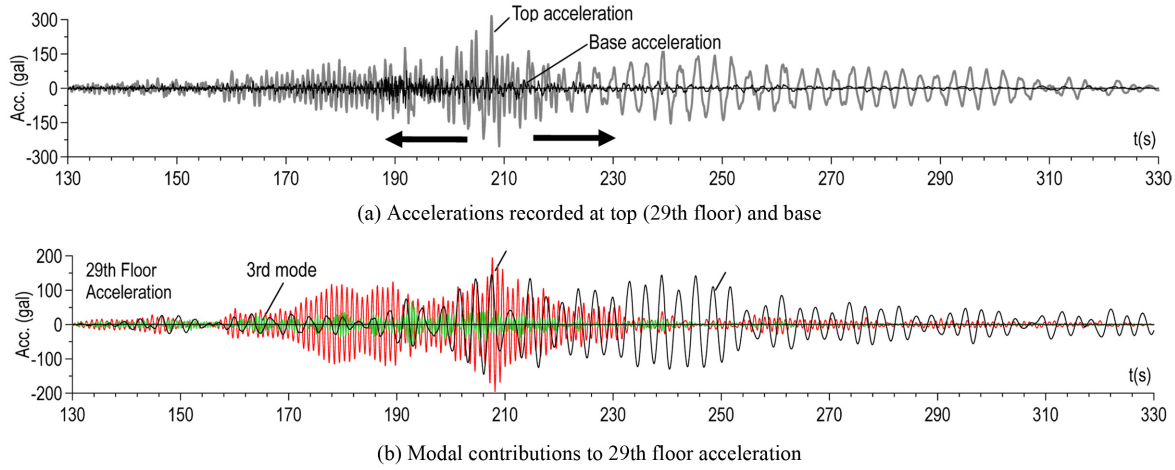


Figure 4. Accelerations (a) recorded at base and 29th floor, and (b) modal contributions at 29th floor.

mode response increased and became dominant. Although not shown, for the 16th floor the 2nd mode was much more dominant, producing almost the same acceleration as top floor. This is due to the 2nd mode vector giving the largest modal responses around the mid-height of the building.

2.2. Damper Types and Vibration Control

Fig. 5 shows schematically the mechanism and hysteresis characteristics, of five major damper types manufactured in Japan. They are called as viscous, oil, viscoelastic, steel, and friction dampers in the order (JSSI, 2003, 2005, 2007, 2013). The first three types are called as the velocity-dependent types, the last two as the deformation-dependent type. Ground accelerations in Tokyo during the 2011 quake was not large enough to cause significant yielding or slipping of the deformation-dependent types, and energy dissipation by the type was none or negligibly small.

This is evidenced by Fig. 6 which shows the transfer function obtained using the acceleration of building top floor and base for the two buildings that are located nearby, hence were subjected to almost the same ground shaking. They are the 38-story building having steel dampers only (Fig. 6(a)), and 37-story building having both steel dampers and viscous dampers (Fig. 6(b)).

The former shows the 1st mode damping ratio 0.017, similar to the value obtained from the 29-story conventional building (Sec. 2.1). On the other hand, the latter showed the 1st mode damping ratio 0.046, about 2.7 times larger. These are understood from wider and lower resonance curves for the latter (Figs. 6(a), 6(b)).

Note that the damping ratio of 0.046 may not sound large to some readers, since the design codes typically use the value 0.05. However, the value of 0.05 is not meant to represent the actual values which, for the steel supertall buildings, are mostly less than 0.02 (AIJ, 2014). Thus, the value 0.046 could lead to reasonably good control.

2.3. Building with Velocity-Dependent Dampers

Kasai et al. discussed performance curve of a variety of vibration-controlled buildings (Kasai et al., 2013) and pro-

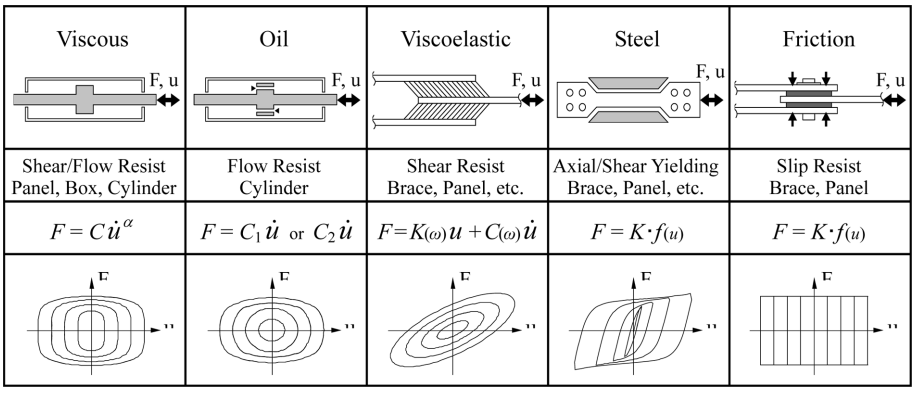


Figure 5. Five major types of dampers used in Japan (JSSI, 2003, 2005, 2007, 2013).

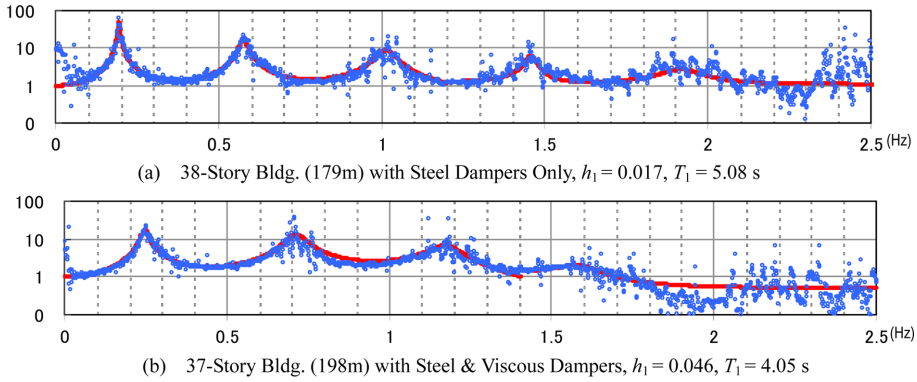


Figure 6. Transfer functions of tall buildings (a) with steel dampers only, and (b) with steel and viscous dampers.

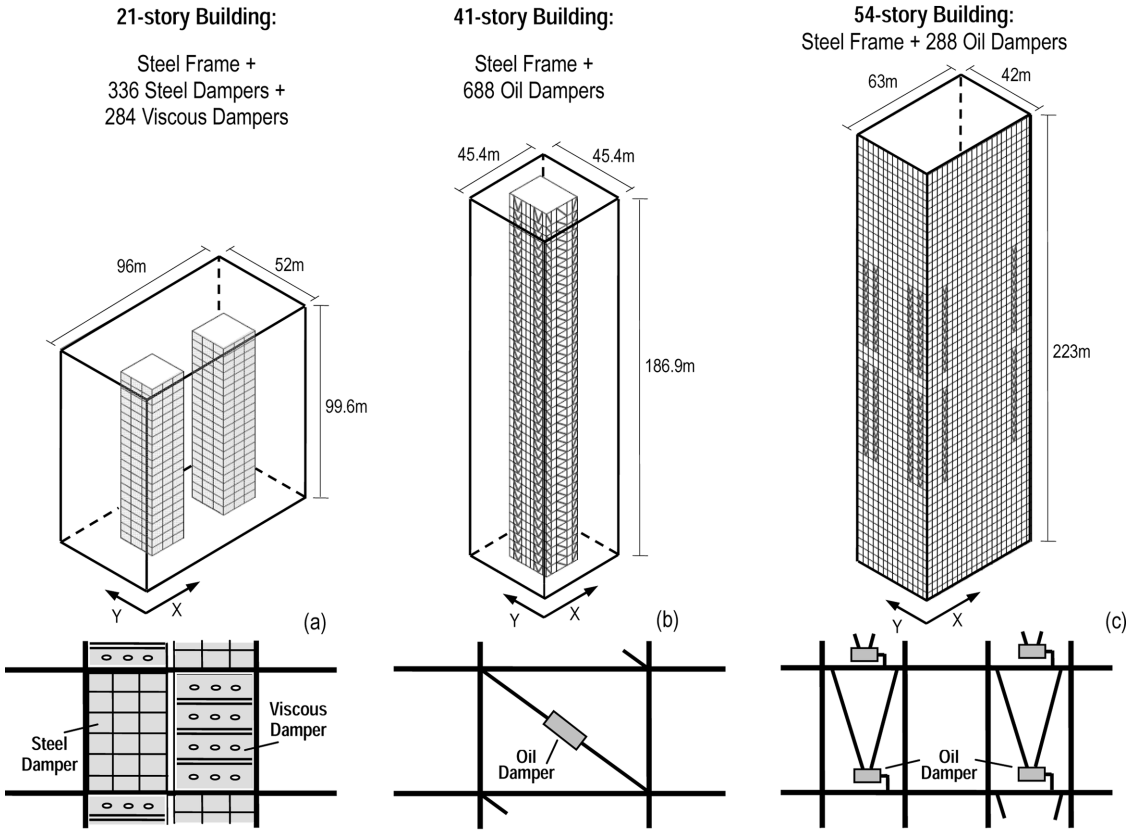


Figure 7. Three response-controlled buildings and dampers.

vided more focused discussions on three tall buildings with velocity-dependent dampers (JSSI, 2003, 2005, 2007, 2013). They are 21, 41, and 54-story buildings as shown in Figs. 7(a), 7(b), and 7(c), respectively.

The 21-story building (Fig. 7(a)) consists of a steel frame and 336 low yield point steel (wall) dampers and 284 viscous (wall) dampers (Koyama and Kashima, 2011; Kasai et al., 2012). In order to overcome the drawback of the steel dampers (Sec. 2.2), viscous dampers are also used, and the steel damper, the most economical among all types is expected to dissipate much energy at the larger quake.

The 41-story building (Fig. 7(b)) consists of a frame using concrete-filled tube columns and steel beams, and 688 oil dampers (Kasai et al., 2012). The relief mechanism to limit the force is provided, but most likely relief did not occur for the level of shaking.

The 54-story building (Fig. 7(c)) has steel frames and was constructed in 1979. It was retrofitted in 2009 (Mas-

eki et al., 2011; Kasai et al., 2012) by attaching 288 oil dampers. 12 dampers per floor were attached to middle 24 stories of the building. The relief mechanism of the oil damper is modified to reduce the axial force of the column and uplift force of the foundation. Most likely, the relief did not occur for the level of shaking.

The maximum ratio of accelerations of top to base in both x- and y-directions was 1.80, 2.38, and 2.51 for the 21, 41, and 54-story buildings, respectively. They are well below the ratio of 3.55 obtained in the conventional 29-story building (Sec. 2.1). The three buildings remained elastic, and the 1st mode damping ratios are about 4%, and those of the 2nd and 3rd modes are almost equal or larger. The 1st mode vibration periods in x- and y-directions are 1.83 s and 1.97 s fot the 21-story building, 3.97 s and 4.10 s for the 41-story building, and 5.37 s and 6.43 s for the 54-story building.

In these three buildings, the trends of the modal contributions are like that of seismically-resistant 29-story building (Sec. 2.1, Fig. 4), but the amplitudes are smaller due to the supplemental damping. Excellent accuracies of the modal properties are confirmed by the modal superposition time-history analyses like those in Sec. 2.1. Then, by intentionally changing the 1st to 3rd mode damping ratios to 0.01, the analyses are repeated.

Example is shown in Fig. 8 for the 41-story building by gray lines. The original responses are considerably smaller (black lines) than those with the hypothetical low damping (gray line). The peak accelerations and displacements are about 0.5 and 0.7 times those of the low damping case. Moreover, between significant ground shakings, the responses decay much faster, and number of large cycles is reduced considerably (Fig. 8). These help reducing damage and fatigue of structural and non-structural component as well as fear or discomfort of the occupants.

2.4. Component Responses in Controlled Building

Non-structural components including equipment cost much more than structural frame, and their damage as well as consequent disruption of business was the main cause for the considerable economic loss by the 2011 Tohoku-Oki Earthquake. Large inertia forces against the non-structural components are produced by the component accelerations, typically much larger than the building floor accelerations (Sec. 2.1).

Fig. 9 shows component acceleration spectra for the top floors of the 29-, 21-, 41- and 54-story buildings. Damping ratio of the component is assumed to be 0.03. The value designated as "Original Bldg. Damping" is the first mode damping ratio. For the 29-story building with conventional structural system (Fig. 9(a)), the broken line is based on the recorded top floor acceleration of the original building, and solid line shows a hypothetical case where the building damping ratios of the first three modes are increased to 0.04. In contrast, for the 21-, 41- and 54-story buildings with dampers (Figs. 9(b)~9(d)), the solid line is based on recorded top floor acceleration of the original building, and the broken line shows hypothetical cases where the first to the third modal damping ratios of the buildings are reduced to 0.01. These show a merit of increased damping for protecting the acceleration-sensitive components.

According to Fig. 9, the past observation that short-period components are safer in a tall building is incorrect. They are as vulnerable as the long-period components due to multiple resonance peaks created by different modes of the building. The peaks are extremely high, even greater than 20 m/s^2 (≈ 2G) for the GPA of 0.6 to 0.8 m/s^2. They may be as high as 8G when the GPA is 4 times, as expected. Note that three peaks for each building are shown in Fig. 9 for the first three modes that could be identified, but more peaks may exist in reality.

The facilities may overturn when floor acceleration exceeds 0.3G, and ceiling whose vibration period typically ranges from 0.3 s to 1 s may fall when its acceleration response exceeds 1G. Fig. 9 also indicates that the building vibration control with damping ratios of about 0.04 is very effective for reduction of the component accelerations over wide range of component periods.

Note also that component displacement relative to the building floor can be estimated as the product of the component accelerations shown and $(T/2\pi)^2$ where T = com-

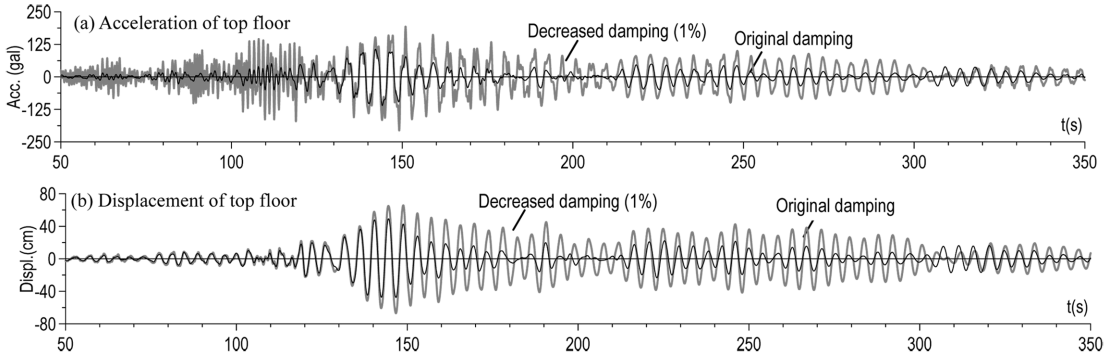


Figure 8. 41-story building with different damping ratios (x-dir.).

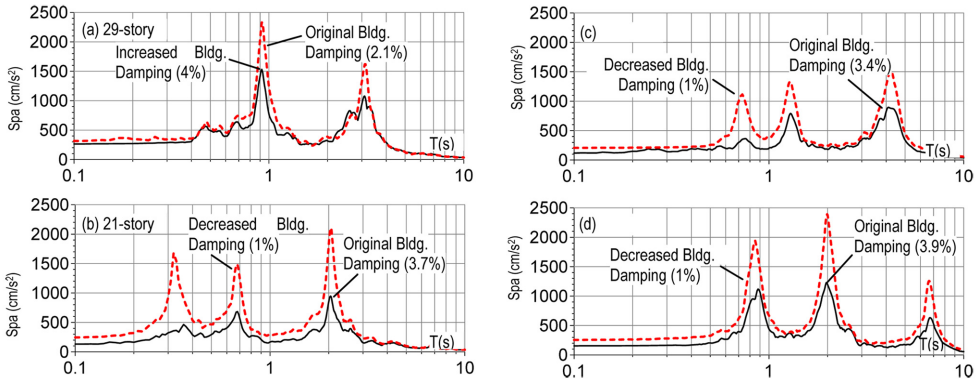


Figure 9. Component response spectra (component damping ratio=3%).

ponent vibration period. Thus, Fig. 9 implies very large component displacements when T is large, which can explain the large motion of the copy machine mentioned earlier (Fig. 3(b)). In this regard, component isolation scheme would require the stroke that is prohibitively long, when using it in the super-tall building.

Considering these, for the super-tall buildings having prominent multi-mode effects, practical methods to mitigate component damage would be; increase of damping ratios for the buildings and/or even components, and; tuning of the component period to avoid multiple resonance peaks (Fig. 9).

3. Progress of Design Methods

3.1. Specifications for Vibration Control

A variety of specifications for vibration control of buildings have been published. Especially, "Design and Construction Manual for Passively Controlled Buildings" (JSSI, 2003, 2005, 2007, 2013) has been the most comprehensive and continuously updated document, covering wide range of damper types and frame types. The "performance curve" and the "displacement-targeted design" have been adopted in several other specifications for vibration control of the steel, concrete, and timber frames.

As one of such example, the AIJ specifications for steel frames with steel dampers (AIJ, 2014) will be explained. Their unique features are as follows:

(1) Methods to evaluate and design dampers, frame members, and connections are given.

(2) Supplemental damping and stiffness effects are expressed on a common scale using a unified theory. (3) Building shorter than 60 m can be designed by using performance curve and static analysis only.

(4) Frame and damper analysis methods are described and subprogram for damper model is given.

As shown in Fig. 10, the specifications provide a simple design route 1 for relatively short steel buildings noted in (3) above, if the displacement-targeted design using performance curve or comparable method is employed to size the dampers (Sec. 3.2). For the taller buildings, detailed check by route 2 or 3, both involving time history analysis, is required. The displacement-targeted design is recommended for preliminary damper sizing for the super-tall buildings as well.

3.2. Displacement-Targeted Design Using Dampers

Using mathematical expressions for the effective vibration period and damping ratio of the building with dampers and idealized seismic response spectra, seismic peak

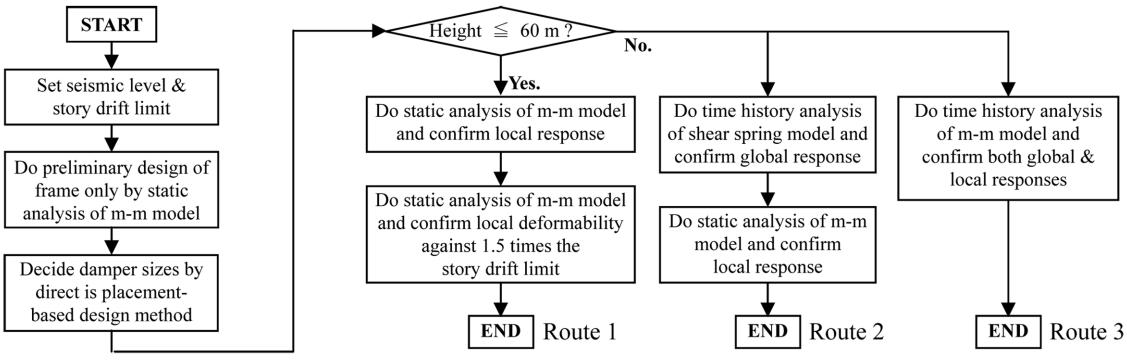


Figure 10. AIJ steel damper and frame specifications ("m-m model" means the member-to-member model).

responses of systems and local members can be expressed by a continuous function of the structural and seismic parameters. The curve plotting the functions is called as "performance curve" which clearly shows differences and commonalities of various systems having different dampers.

Since publication of performance curves for steel and viscoelastic dampers (Kasai et al., 1998; Fu & Kasai, 1998), the concepts and methods have been confirmed by other parties, and expanded to include higher mode vibrations, frame yielding with different hysteretic characteristics, and more damper types (e.g., Kasai et al., 2005, 2006, 2007, 2008). To-date, the performance curves have been adopted by six different design specifications in Japan for vibration control of steel, concrete, and timber frames.

Fig. 11 shows the performance curve for the steel, viscous, oil, and viscoelastic dampers combined with an elastic frame. The curve considers an equivalent single-degree-of-freedom (SDOF) system and shows the displacement reduction ratio R_d and force (or pseudo-acceleration) reduction ratio R_{pa} expressed relative to the frame responses without dampers.

As an example, the curves in the left upper figure shows the steel damper case, and theoretically reflects effects of the stiffness ratio K_a/K_f between the added component and frame, and ductility demand μ of the added component, where the added component is a damper and brace combined in series. Fig. 11 assumes constant pseudo-velocity spectrum, but other cases can also be plotted. The curves clearly indicate the effects of the parameters. They also give necessary K_a/K_f and μ values for the target drift or R_d value. Required yield force of the damper is also obtained from the R_d and R_a values. Once the necessary K_a/K_f value in the SDOF system is obtained, it is converted to the dampers in the multi-story system whose frame stiffness is explicitly known at each story.

The performance curves for the other dampers can be used in a similar manner. They enable the displacement-target or even acceleration-target design of the vibration-controlled building. A special method is also given in specifications for assuring reasonably uniform story drift distributions, even when the frame tends to deform non-uniformly.

Fig. 11 also shows prediction of peak responses for the full-scale 5-story building specimen tested at the E-Defense facility, Miki City in Japan (Kasai et al., 2009a, 2009b; Ooki et al., 2009). Four cases using the above-mentioned dampers were tested, and the JR Takatori ground motion recorded during the 1995 Kobe earthquake was used. Black and white symbols show prediction and test results, respectively, and they are plotted for the table motions scaled to 15% and 100% of the Takatori motion, respectively. The prediction appears to be reliable.

Currently, the prediction is extended to much taller buildings, and has been validated through numerical experiments.

3.3. Methodogies for Retroft Design

Various mitigation measures including seismic retrofit are being investigated for older super-tall buildings in Japan. This will be explained below, by referring to a project in which the wpriter is involved:

The example is a seismically-resistant 29-story steel building explained in Sec. 2.1 (Fig. 2). The research team

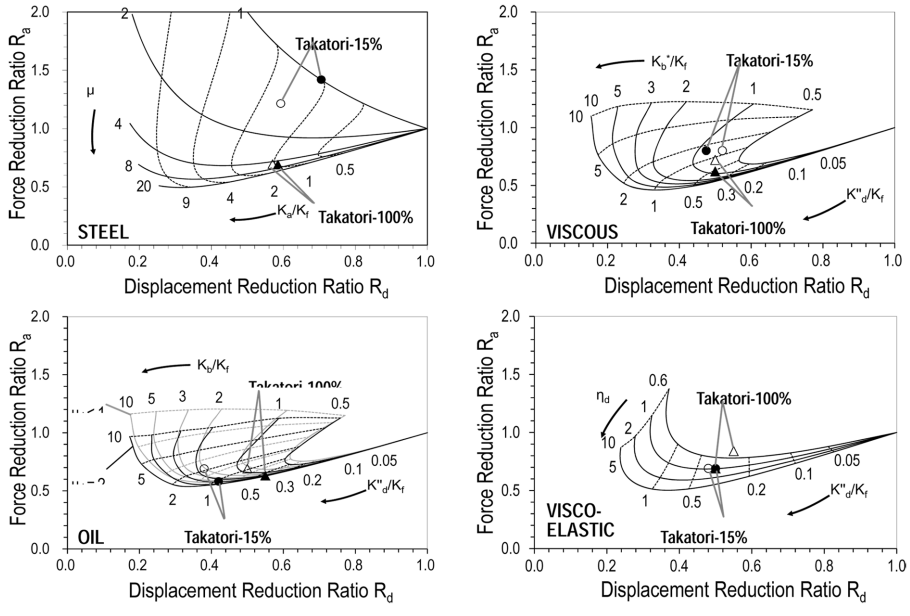


Figure 11. Performance Curves for four damper types and comparison with E-Defense test results (White Symbols: Test Results, Black Symbols: Predictions).

at Kogakuin University formulated a member-to-member analytical model of this building. The model is found to simulate the recorded responses (Sec. 2.1) with reasonable accuracy. The building consists of steel moment resisting frames combined with many short braces providing seismic resistance. The slenderness of the typical brace is about 50, and buckling capacity is relatively large. However, since the braces yield at small story drift, their maximum deformation and cumulated plastic deformations must be controlled in order to avoid significant deteriorations of strength and stiffness.

Analysis uses two artificial long period ground motions simulating phases of the basement accelerations recorded during the 2004 Kiihanto-Oki earthquake and the 2001 Tohoku-Oki earthquake, respectively. The former has about 500 second duration of shaking. Another artificial earthquake, large pulse ground motion from hypothetical Tokyo near-field earthquake, and the 1940 El Centro earthquake (NS) that is scaled 1.495 times (i.e., peak ground acceleration 0.521 g) to satisfy peak ground velocity of 50 cm/s are used. The scaled El Centro earthquake is one of the major earthquakes considered for the level 2 seismic design of tall buildings in Japan.

In a building with dampers, the frame must have the ability to transmit its deformation and inertia force to the damper as much as possible in order to maximize energy dissipation by the damper. The appropriate damper locations are found by conducting elastic analysis of the frame without damper and by measuring the magnitude of shear drift of frame unit. The lateral force distributions agrees with those from the so-called *Ai*-distributions stipulated by the Japanese code.

Fig. 12 shows story drifts of the building and shear drifts of the frame units of interest. For the NS direction (Fig. 12(a)), the frame units in the central bay are considered, since their shear drifts would be amplified by the significant chord (bending) drifts of existing brace bays at both sides. As Fig. 12(a) shows, shear drift of the central bay unit is larger than the story drift of the building, suggesting possibility of large damper stroke and energy dissipation. Note that the 2nd and 6th bays are alternatively checked and their shear drifts are found to be much smaller.

As for the EW direction (Fig. 12(b)), the dampers are attached at the one-quarter span of the 25.6 m long beam of 1 m depth. Due to the eccentric attachment of the damper, large shear deformation develops (Fig. 12(b)), where triangle is formed by the two dampers (Fig. 13).

In order to control vibration for smaller earthquake and to limit the damper forces for larger earthquake, the oil damper with relief mechanism is used (Fig. 14). The damper price is only 20% of the total retrofit cost of about $100,000 per location, including structural, and largely non-structural and cosmetic works. Thus, limiting the number of dampers locations is a key to control the cost. All the oil dampers have common sizes and properties of relief load F_{dy}=1,600 kN, viscous coefficient C_d=375 kN/(cm/s), post-relief viscous coefficient pC_d=37.3 kN/(cm/s), and damper stiffness K_d=5,400 kN/cm (Figs. 13 and 14).

3.4. Retrofit Using Minimum Amount of Dampers

Fig. 15 shows two retrofit designs: D32 design uses 32 dampers for NS and EW directions in total. D64 design uses 64 dampers. More dampers are used for the NS direction, considering smaller shear drift (≃ damper stroke horizontal component) compared with the EW direction (Fig. 12). The story for the damper installation is selected in the order from the largest shear drift of the frame unit, but selection of consecutive story is avoided. The example selections for the D32 design are shown by the horizontal broken lines drawn in earlier Figs. 12(a) and 12(b). For both D32and D64 designs in NS direction (Fig. 15), since

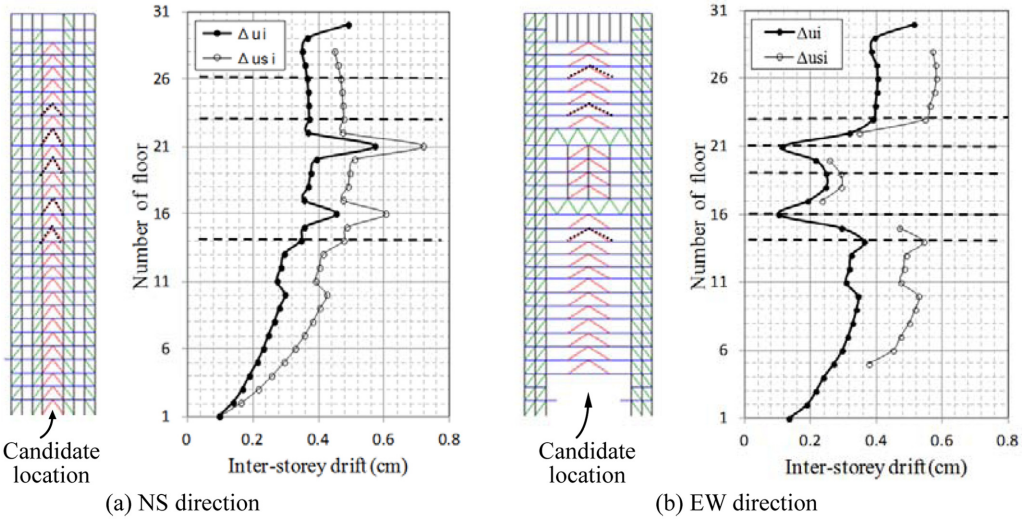


Figure 12. Static analysis to find deformation mode: Comparison between building story drift and frame unit shear drift.

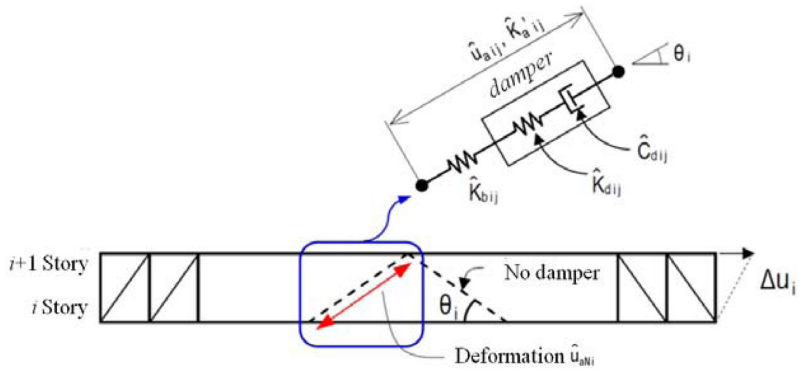


Figure 13. Candidate location of the dampers in the EW frame (Fig. 12b).

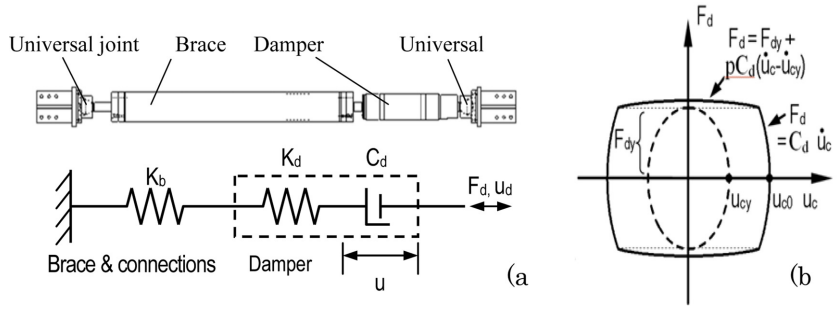


Figure 14. (a) Oil damper considered and analysis model; and (b) hysteresis curves under smaller and larger strokes.

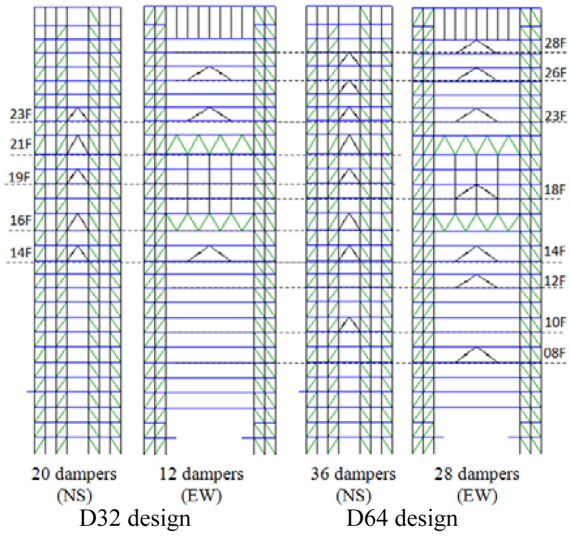


Figure 15. Location of the dampers: D32 (=20+12) design and D64 (=36+28) design.

the 21st level tends to show the largest frame unit shear drift without dampers, 8 dampers instead of 4 dampers are considered.

Thus, D32 design considers in average 0.68 and 0.41 dampers per story in the NS and EW directions, respectively. Whereas, D64 design considers 1.24 and 0.97 dampers per story. In spite of these small numbers, D32 design gives damping ratios of 0.036 and 0.040 in the NS and EW directions, respectively, and D64 design gives 0.052 and 0.054, respectively, as estimated from free vibration analyses. The small numbers of retrofit locations and yet relatively large damping ratio indicate the design is very economical and efficient.

Figs. 16, 17, and 18 show displacements, story drifts, and accelerations due to the aforementioned artificial earthquake with the phase of the 2001 Tohoku-Oki earthquake. By virtue of increased damping ratios, both D32 and D64 design show good vibration control: it suggests significant drift reduction by using less than one damper per story for each horizontal direction. The peak floor accelerations did not show such reduction, but the time history indicated excellent reduction of number of large response cycles and duration of significant shaking of the building (see also Sec. 2.2).

The response reduction effect of D32 design relative to non-retrofit case can be considered significant, compared with the effect of D64 design. In this manner, it is important to recognize the range of effectiveness is largely affected by the given frame that is not originally designed for damper installations.

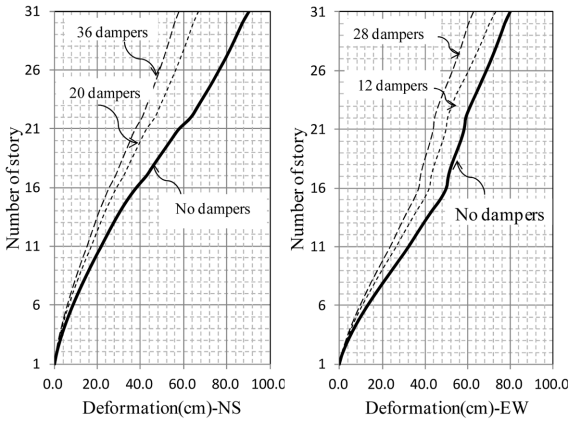


Figure 16. Displacements with/without dampers.

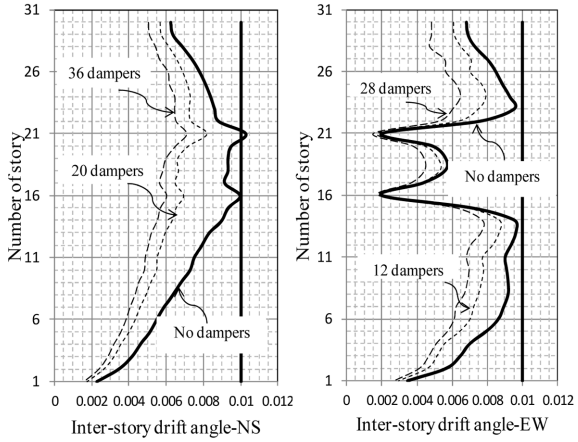


Figure 17. Inter-story drift angle with/without dampers.

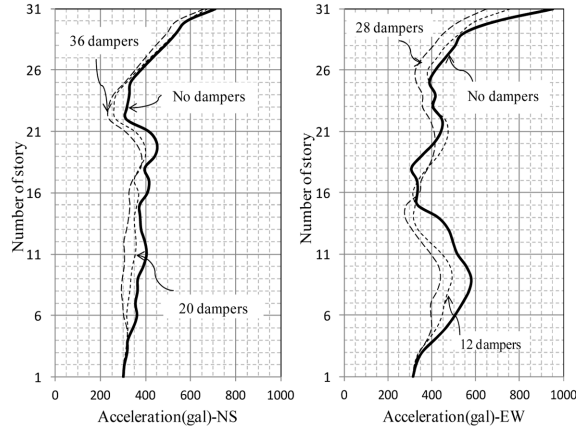


Figure 18. Accelerations with/without dampers.

Note also the earthquake shows constant spectral velocity of 80 cm/s at damping ratio of 0.05 for the moderate to long vibration periods. This is about 30% less than the El Centro motion amplified to level 2 at the buildings vibration periods of about 3 sec. in both EW and NS directions. But duration of shaking is much longer. Due to the limited page length, more discussions will be presented in the writer's lecture, regarding the required ductility ratio and cumulated plastic deformations of the beams and braces, which largely vary according to types of the earthquakes.

4. Summaries and Conclusions

Due to the recent seismic hazards, Japan's focus on seismic hazard mitigation for super-tall buildings has clearly shifted to resilience and continued functionality of the buildings against major seismic attacks.

Numerous super-tall buildings in Tokyo, when subjected to the expected shaking three to four times stronger than the 2011 Tohoku-Oki earthquake, must be robust enough to keep functioning and preventing socio-economic loss, and not produce many commuter worker evacuees who will hardly find havens locally.

This paper, therefore, first analyzed and contrasted performance of the super-tall buildings with/without the protective systems based on the responses recorded during the 2011 quake, and evaluated current state of vibration control effectiveness. The efforts of specification developments as well as research to enhance effectiveness of the protective systems are explained.

The records and survey reports also indicated the need for mitigation of acceleration-induced hazards in the super-tall buildings. The use of dampers appears to be desirable, since it can reduce not only peak accelerations but also number of large response cycles, and duration of significant shaking of the building.

The present paper also has addressed retrofit of the super-tall buildings constructed prior to the 1985 Kobe earthquake. The buildings are mostly conventional steel frames without dampers. Their retrofit project by incorporating dampers is underway, and an example was demonstrated in the present paper.

Acknowledgements

The writer acknowledges the contributions provided by Prof. Du, Nanjing University of Technology, Prof. Pu, Wuhan University of Technology, Prof. Yamashita, Prof. Hisada, Mr. Shirasaki, Ms. Aoki, and Ms. Nakanishi of Kogakuin University, and Prof. Matsuda, Tokyo Institute of Technology.

References

AIJ. (2014) *Design Specifications on Steel Frame and Damper* Nov. (in print, in Japanese).

Fu, Y. and Kasai, K. (1998) "Comparative Study of Frames

Using Viscoelastic and Viscous Dampers", *J. Struct. Eng., American Society of Civil Engineers*, 122(10), 513-522.

Hisada, Y., Yamnashita, T., and et al. (2012) "Seismic Response and Damage of High-Rise Buildings in Tokyo, Japan, during the 2011 Tohoku Earthquake", *Proceedings, 15WCEE*, Lisbon, Portugal.

JSSI (2003, 2005, 2007, 2013) *Design and Construction Manual for Passively Controlled Buildings*, Japan Society of Seismic Isolation, Tokyo (in Japanese).

Kasai, K., Fu, Y., and Watanabe, A. (1998) "Passive Control Systems for Seismic Damage Mitigation," *Journal of Structural Engineering, American Society of Civil Engineers*, 124(5), 501-512.

Kasai, K. and Ito, H. (2005) "Passive Control Design Method Based on Tuning of Stiffness, Yield Strength, and Ductility of Elasto-plastic Damper," *J. Struct. Constr. Eng., AIJ*, 70(595), 45-55. (in Japanese)

Kasai, K., Minato, N., and Kawanabe, Y. (2006) "Passive Control Design Method Based on Tuning of Equivalent Stiffness of Visco-elastic Damper," *J. Struct. Constr. Eng., AIJ*, 71(610), 75-83. (in Japanese)

Kasai, K., Ogura, T., and Suzuki, A. (2007) "Passive Control Design Method Based on Tuning of Equivalent Stiffness of Nonlinear Viscous Damper," *J. Struct. Constr. Eng., AIJ*, 72(618), 97-104. (in Japanese)

Kasai, K., Ito, H., and Ogura, T. (2008) "Passive Control Design Method Based on Tuning of Equivalent Stiffness of Bilinear Oil Damper," *J. Struct. Constr. Eng., AIJ*, 73 (630), 1281-1288. (in Japanese)

Kasai, K., Motoyui, S., Ozaki, H., Ishii, M., Ito, H., Kajiwara, K., and Hikino, T. (2009a) "Full-Scale Tests of Passively-Controlled 5-Story Steel Building Using E-Defense Shake Table, Part 1: Test Concept, Method, and Building Specimen," *Proc. of STESSA 2009*, Keynote Paper, pp. 11-17, Philadelphia.

Kasai, K., Ooki, Y., Ito, H., Motoyui, S., Hikino, T., and Sato, E. (2009b) "Full-Scale Tests of Passively-Controlled 5-Story Steel Building Using E-Defense Shake Table, Part 2: Preliminary Analysis Results," *Proc. of STESSA 2009*, pp. 87-92, Philadelphia.

Kasai, K., Pu, W., and Wada, A. (2012) "Responses of tall buildings in Tokyo during the 2011 Great East Japan Earthquake," Keynote Paper, *Proc. STESSA 2012*, pp. 25-35, Santiago, Chili.

Kasai, K., Mita, A., Kitamura, H., Matsuda, K., and et al. (2013) "Performance of Seismic Protection Technologies during the 2011 Tohoku-Oki Earthquake," *Earthquake Spectra*, 29(S1), S265-S293, March.

Koyama, S. and Kashima, T. (2011) "Prompt Report on Strong Motions Recorded during the 2011 Tohoku Pacific Ocean Earthquake, Report 5," *Building Research Institute (BRI)*.

Maseki, R., Nii, A., Nagashima, I., Aono, H., Kimura, Y., and Hosozawa, O. (2011) "Performance of Seismic Retrofitting of Suoer High-Rise Building Based on Earthquake Observation Records," *International Symposium on Disaster Simulation and Structural Safety in the Next Generation* (DS'11), Japan.

Ooki, Y., Kasai, K., Motoyui, S., Kaneko, K., Kajiwara, K., and Hikino, T. (2009) "Full-Scale Tests of Passively-Controlled 5-Story Steel Building Using E-Defense Shake Table, Part 3: Full-Scale Tests for Dampers and Beam-Column Subassemblies," *Proc. of STESSA 2009*, pp. 93-99, Philadelphia.